



## Preparing a celadonite electron source and estimating its brightness

E. Salançon, Alain Jean Degiovanni, Laurent Lapena, Roger Morin

### ► To cite this version:

E. Salançon, Alain Jean Degiovanni, Laurent Lapena, Roger Morin. Preparing a celadonite electron source and estimating its brightness. Journal of visualized experiments: JoVE, 2019, 153, 10.3791/59513 . hal-02359792

**HAL Id: hal-02359792**

**<https://amu.hal.science/hal-02359792>**

Submitted on 12 Nov 2019

**HAL** is a multi-disciplinary open access archive for the deposit and dissemination of scientific research documents, whether they are published or not. The documents may come from teaching and research institutions in France or abroad, or from public or private research centers.

L'archive ouverte pluridisciplinaire **HAL**, est destinée au dépôt et à la diffusion de documents scientifiques de niveau recherche, publiés ou non, émanant des établissements d'enseignement et de recherche français ou étrangers, des laboratoires publics ou privés.

**TITLE:**

**Preparing a celadonite electron source and estimating its brightness**

**AUTHORS & AFFILIATIONS:**

Evelyne Salançon, Alain Degiovanni, Laurent Lapena and Roger Morin

CINaM

Aix-Marseille Univ., CNRS, UMR 7325

Campus de Luminy-case 913

13288 Marseille Cedex 9

Evelyne Salançon: [salancon@cinam.univ-mrs.fr](mailto:salancon@cinam.univ-mrs.fr)

Phone: (+33)6 60 36 28 05

Alain Degiovanni: [degiovanni@cinam.univ-mrs.fr](mailto:degiovanni@cinam.univ-mrs.fr)

Laurent Lapena: [lapena@cinam.univ-mrs.fr](mailto:lapena@cinam.univ-mrs.fr)

Roger Morin: [morin@cinam.univ-mrs.fr](mailto:morin@cinam.univ-mrs.fr)

**KEYWORDS:**

Unique crystal deposition; low-energy electron point-source; field emission; brightness estimation; electron holography; electron microscopy

**SHORT ABSTRACT:**

The article presents a protocol to prepare the celadonite source and estimate its brightness for use in a long-range imaging low-energy electron point-source projection microscope.

**LONG ABSTRACT:**

The electron celadonite source described in this article performs well in a low-energy electron point-source projection microscope in long-range imaging. It presents major advantages compared to sharp metal tips. Its robustness affords a lifetime of months and it can be used under relatively high pressure. The celadonite crystal is deposited at the apex of a carbon fiber, maintained itself in a coaxial structure ensuring a spherical beam shape and easy mechanical positioning to align the source, the object and the electron-optical system axis. There is a single crystal deposition via generation of celadonite-containing water droplets with a micropipette. Scanning electron microscopy observation can be performed to verify the deposition. However, this adds steps and therefore increases the risk of damaging the source. Thus, after preparation, the source is usually inserted directly under vacuum in the projection microscope. A first high voltage supply provides the kick-off needed to start the electron emission. The field emission process involved is then measured: it has already been observed for dozens of electron sources prepared in this way. The brightness is under-estimated through an over-estimation of source size, intensity at one energy and cone angle measured in a projection system.

## INTRODUCTION:

Metal/insulator structures used for electron emission have been studied for almost 20 years due to their low macroscopic field [1]. The electric field involved is only of the order of some V/ $\mu\text{m}$  [2,3,4], in contrast to the V/nm required for classic field emission with sharp metal tips [5,6,7]. This probably explains the starting plasma discharges that are so useful in electron source technologies. Some years ago, we sought to explore this low field emission by depositing films of natural insulators on electron transmission carbon layers [8]. Celadonite, an insulator mineral found in the basalt of the Parana Traps in the mines of Ametista di Sul in Brazil, was chosen.

When celadonite is ground, the crystal shape is a rectangular slab with micrometric dimensions and a thickness of less than 100nm (typically: 1000nm $\times$ 500nm $\times$ 50nm). It is perfectly flat and recognizable in scanning electron microscopy (figure 1). The film is formed by deposition of a celadonite-containing water droplet on the carbon layer. As applied voltage increases, it emits electrons following a Fowler-Nordheim regime with intensity saturation for the highest voltages. A study using a diaphragm in a projection system showed that one emitter is a point-like source [9]. However, using this large film with a diaphragm to select the source did not exploit the potential of the point-source. For example, the point-sources commonly used in low-energy electron point-source projection microscopy allow a source-to-object distance of about 100nm. However, such a source-to-object distance would be out of the question with a film. Finding a way to isolate one crystal so as to be able to move something towards this electron source was a challenge. Our solution was first, to use a 10 $\mu\text{m}$  carbon fiber: depositing the droplet at the apex of the fiber necessarily limits the number of celadonite crystals. Second, we decided to limit droplet size: a micropipette with a tip end of about 5 $\mu\text{m}$  is filled with celadonite-containing water and pressure is applied at the entrance of the micropipette to create a small drop to wet the apex of the fiber. The Protocol details the full source preparation process.

The resulting source is a coaxial point-source allowing good alignment between the source, the object and the electron optical system [10]. Because its 10 $\mu\text{m}$  diameter is still wider than ultra-sharp tips the source-to-object distance is limited to some tens of micrometers. However, we recently showed that the celadonite source emitter combined with an Einzel lens performs comparably to a classic point-source projection microscope. The long-range imaging thus made accessible even limits the charge effect [11] on the object and the image distortions involved [12, 13]. The celadonite source also presents major advantages compared to sharp metal tips. It is robust: the point-source is under the crystal and thus protected against sputtering. The source can operate under relatively high pressure: it was tested at 10<sup>-2</sup>mbar during some minutes. Yet its lifetime and its stability remain dependent on the right vacuum conditions. We usually employ the celadonite source at 10<sup>-8</sup>mbar and obtain a lifetime of months.

This video protocol is intended to help all those wishing to realize the celadonite source to produce a coherent electron beam.

## PROTOCOL:

### 1. Preparation of the source

In our microscope, the source-support is composed of a machinable glass ceramic plate from which emerges 1cm of a stainless steel tube of 90 $\mu$ m internal diameter with an electrical connection on the plate.

#### 1.1. Preparation of the fiber

1.1.1. Fix the source support under an optical microscope.

1.1.2. Insert the 10 $\mu$ m carbon fiber into the stainless steel tube.

1.1.3. Glue the carbon fiber to the tube with silver lacquer.

1.1.4. Cut the fiber with a cutting tweezers (under a binocular microscope) so that between 100 $\mu$ m and 3mm are left outside the stainless steel tube.

NB: the carbon fiber is brittle; leaving more than 1cm outside the tube will increase the chance of the structure breaking during manipulation.

#### 1.2. Celadonite-containing water preparation

1.2.1. Grind the celadonite with a mortar and pestle

1.2.2. Weigh 0.2mg of celadonite powder

1.2.3. Dilute this 0.2mg of celadonite in 10ml of deionized water

1.2.4. Use an ultrasound tip directly in the 10ml celadonite-containing water to break the aggregates. We use a typical ultrasonic frequency of 30kHz for a power of 50W during 30s.

#### 1.3. Preparation of the deposition environment

1.3.1. Connect a capillary holder to a pressure controller

1.3.2. Maintain the capillary holder under an optical microscope with a multidirectional micro-manipulator

1.3.3. Place the support with the carbon fiber facing the capillary holder under the optical microscope.

#### 1.4. Celadonite deposition

**1.4.1.** Pull a micropipette with an internal-end diameter of 2 to 10 $\mu$ m to allow the dispersed celadonite to flow without obstruction.

**1.4.1.1.** Fix a glass capillary in the puller jaw.

**1.4.1.2.** Ensure the right puller parameters according to patch pipette size (table 1).

**1.4.1.3.** Fill the micropipette with the celadonite-containing water.

**1.4.2.** Mount the micropipette on the capillary holder under the microscope.

**1.4.3.** Align the micropipette and the carbon fiber under the optical microscope

**1.4.4.** Approach the micropipette, to a distance of 2 to 10 $\mu$ m from the apex of the carbon fiber.

**1.4.5.** Apply progressive pressure on the wide entry to the micropipette. Typically, apply P=100mbar so that a drop forms at the tip but does not fall.

**1.4.6.** This drop wets the apex of the carbon fiber

**1.4.7.** Retract the micropipette

## **2. Kicking-off the source**

In our microscope, the source-support is fixed on a manual rotating flange also carrying the piezo-electric actuator that moves (100nm resolution, 25mm range), with an electrical command, the object relative to the source (See Figure 2). This object plays the role of an electrical anode for electron emission; it is generally electrically grounded and placed in front of the source. In our experiment, voltages are hand controlled with different power supplies.

**2.1.** Install the source holder under vacuum.

**2.2.** Connect the carbon fiber and the object to two high-voltage electrical feedthroughs.

**2.3.** Check electrical continuity of contacts everywhere: anode-object, lens and screen; turn on the vacuum pumping.

**2.4.** Connect a nano-ammeter of a caliber in the  $\mu$ A range between the object and the electrical ground.

**2.5.** Increase the negative bias voltage applied to the source slowly, at approximately 1V/sec. If the anode is 1mm away from the source, the kick-off takes place at about 2kV. Intensity suddenly increases.

**2.6.** Decrease the voltage to stabilize the intensity at some hundred nA. At the beginning, intensity can fluctuate over several orders of magnitude.

**2.7.** Leave the system fluctuating for several hours, until fluctuations decrease. Cut off the voltage when fluctuations are lower than 10%.

### **3. Source characterization**

We expose a way to probe the source capabilities. To estimate the source brightness, two projection microscopes are used. In these setups, the shadow of an object is observed on a fluorescent screen placed farther away (figure 2). The source (cathode) and the object (anode) are mounted on a micro-manipulation flange and can rotate together in the projection plane. A simple short projection setup with a fluorescent screen allows for low magnification projection. The second setup involves an electrostatic lens and a dual microchannel-plate / fluorescent screen assembly for the strongest magnifications [12]. In fact, information available on each projection image is used to under-estimate the brightness: the smallest detail in the record [13]. This smallest visible detail depends on the apparent source-size, that includes the source-size geometrical blur, the vibrations between the object and the source, and detector resolution limits.

#### **3.1. Measurement of the cone angle**

**3.1.1.** Turn the source towards the simple projection setup, with the rotating flange, to observe the electron beam.

**3.1.2.** Decrease the source-to-screen distance, with the manual micro-manipulator, to obtain the entire spot on the screen; then, measure the source-to-screen distance,  $D$ .

**3.1.3.** Take pictures of the screen by changing the angle between the electron beam and the normal to the screen, with the rotating flange.

**3.1.4.** Plot the gray-level intensity profile along one axis and determine the emission radius,  $R$  at a given source-to-screen distance,  $D$  (figure 3).

**3.1.5.** Calculate the cone angle:  $\Omega = \frac{\pi R^2}{D^2}$  with  $R$ , the emission radius at a given source-to-screen distance,  $D$ .

#### **3.2. Measurement of the Fowler-Nordheim plot**

**3.2.1.** Measure the emission intensity versus the voltage applied to the source:  $I(V)$  with  $I$  the intensity measured at the anode and  $V$  the voltage applied at the carbon fiber.

**3.2.2.** Plot  $\ln\left(\frac{I}{V^2}\right) = f\left(\frac{1}{V}\right)$ . The curve shows a decreasing straight line with saturation for highest voltage. An example is given in figure 4. The longest straight line is the signature of the field emission process.

### 3.3. Measurement of the source size

**3.3.1.** Turn the source towards the electrostatic lens, with the rotating flange.

**3.3.2.** Produce a projection image containing a huge Fresnel diffraction pattern along an edge of an object: magnification of about  $G \approx 20,000$  is required. In our microscope, this is possible with a source-to-object distance of some  $100\mu\text{m}$ , fixed with the piezo-actuators, and an Einzel electrostatic lens.

**3.3.3.** Measure the sharpest visible detail on the image on the screen (figure 5)  
NB : The sharpest fringe-to-fringe distance,  $\delta$ , is used.

**3.3.4.** Calculate the source size:  $s = \frac{\delta}{2G}$

### REPRESENTATIVE RESULTS:

Several scanning electron micrographies of carbon fibers prepared as detailed in Protocol were obtained in an SEM from JEOL (JSM-6340F) at 15kV. Sources exhibit one, sometimes two, crystals at their apex (figure 1). However the use of the SEM involves another support for the carbon fiber, hard to mount and demount without breaking. It is safer to attempt direct electron emission. Tested in a projection microscope (figure 2), every source prepared this way emitted. The kick-off is required only once. With old sources, sometimes, a kick-off can be used for another source.

Most of these sources show one single point source (figure 3): the emission profile indicates only one continuing image without any other spot. The beam has a cone angle of about  $1\text{sr}$ . The Fowler-Nordheim plot exhibits 10 orders of magnitude straight and saturation at higher voltage (figure 4). The saturation regime obtained for a given voltage depends on the structure, but the slope decreases systematically for higher current intensities from about  $10\mu\text{A}$ .

Energy distribution is not measured here, because the energy resolution is not good enough to obtain better accuracy than a few eV by simple biasing the entrance of the detector. Another point is that highly structured fringe patterns can be observed in some holograms rejecting a large energy distribution that would blur such patterns. Since the process involved is the Fowler-Nordheim regime, energy distribution close to  $250\text{meV}$  is expected [14].

The source size is estimated by measuring the smallest detail on the image produced. This image is the Fresnel diffraction pattern of the object. Here, loss of interference fringes is attributed to the size of the source (figure 5); this is a way to over-estimate this measurement.

In this case, the source radius is smaller than  $4\text{nm}$  ( $s = \frac{\delta}{2G} = \frac{245\mu\text{m}}{2 \times 18000} = 6.8\text{nm}$ ). Finally, the brightness of the source is obtained,  $B = \frac{I(E \pm \Delta E)}{\Omega \cdot S} = \frac{10\mu\text{A}}{1\text{sr} \times \pi \times 12 \times 10^{-14}\text{cm}^2} = 3 \cdot 10^7 \text{A} \cdot \text{cm}^{-2} \cdot \text{sr}^{-1}$ .

The method presented here under-estimates this brightness.

#### **DISCUSSION:**

This protocol is not critical because the geometry of a source at a microscopic scale changes from one source to another one. Difficulty is that since a carbon fiber is brittle, its cutting can lead to inappropriate length. Adequate length is about 500 $\mu\text{m}$ , the microscopic shape of the cut is not crucial. The critical step is to have a very small number of crystals (ideally one) deposited on the apex of a conductive wire. Adapting the crystal concentration with the deposited volume is the most important point. If too many crystals aggregate, emission is damped. Here we describe a way to manage this. Due to the kick-off procedure, if a small number of crystals is deposited only one of them is finally responsible for the emission. Another requirement is to build a protruding structure in order to approach the anode and to obtain a directive emission. This cannot be achieved if celadonite-crystals were deposited on a carbon film as in previous studies.

The electron celadonite source is now regularly used in a low-energy electron point-source projection microscope, associated with an Einzel lens system. Because of the high brightness of the source, at this large working distance of 600 $\mu\text{m}$ , a resolution of about 30nm is generally obtained [12]. In point-projection microscopes, working at a so large source-object distance is comfortable and is really advantageous. Moreover, such large working distances avoid any field effect on the object. The high emission intensities provided by this source enable image acquisition at a video rate of about 500images/sec, and the robustness of the source is a practical advantage over classic field emission metal tips. Except in our microscope this recently developed source has not yet been used in another microscope. The emission instabilities previously measured could be problematic for a scanning microscope. Although these instabilities are observable during point-projection imaging, the emission location is stable, making image averaging possible. Compared to classic metal-tip sources for identical magnification, holograms obtained with present source are identical but obtained for a much larger working distance. Ultimate spatial resolution is presently an open experimental problem.

#### **ACKNOWLEDGMENTS**

The authors would like to thank Marjorie Sweetko for improving the English of this article.

#### **DISCLOSURES**

The authors have no competing financial interests.

#### **REFERENCES:**

- [1] - Forbes, R.G. Low-macroscopic-field electron emission from carbon films and other electrically nanostructured heterogeneous materials: hypotheses about emission mechanism, *Solid-State Electronics* 45, 779-808 (2001)
- [2] - Wang, C., Garcia, A., Ingram, D.C., Lake, M, Kordesch, M.E. Cold field emission from CVD diamond films observed in emission electron microscopy, *Electronics Letters* 27, 1459 (1991)
- [3] - Okano, K., Koizumi, S., Ravi, S., Silva, P., Amaratunga, G. Low-threshold cold cathodes made of nitrogen-doped chemical-vapour-deposited diamond, *Nature* 381, 140-141 (1996)
- [4] –Geis, M.W. et al., A new surface electron-emission mechanism in diamond cathodes,



*Nature* 393, 431-435 (1998)

[5] - Horch, S., Morin, R. Field emission from atomic size sources, *Journal of Applied Physics* 74(6), 3652-3657 (1993)

[6] - Muller, H.U., Volkel, B., Hofmann, M., Woll, C., Grunze, M. Emission properties of electron point sources, *Ultramicroscopy* 50(1), 57-64 (1993)

[7] - Qian, W., Scheinfein, M.R., Spence, J.C.H. Brightness measurements of nanometer-sized field-emission-electron sources, *Journal of Applied Physics* 73(11), 7041-7045 (1993)

[8] - Rech, J., Grauby, O., Morin, R., Low-voltage electron emission from mineral films, *Journal of Vacuum Science & Technology B* 20(1), 5-9 (2002)

[9] - Daineche R., Degiovanni A., Grauby O., Morin, R. Source of low-energy coherent electron beams, *Applied Physics letters* 88, 023101 (2006)

[10] - Salançon, E., Daineche, R., Grauby, O., Morin, R. Single mineral particle makes an electron point source, *Journal of Vacuum Science & Technology B* 33, 030601 (2015)

[11] - Prigent, M., Morin, P. Charge effect in point projection images of Ni nanowires and I collagen fibres, *Journal of Physics D: Applied Physics* 34(8), 1167-1177 (2001)

[12] - Salançon, E., Degiovanni, A., Lapena, L., Lagaize, M., Morin, R., A low-energy electron point-source projection microscope not using a sharp metal tip performs well in long-range imaging, *Ultramicroscopy* 200, 125-131 (2019)

[13] – Salançon, E., Degiovanni, A., Lapena, L., Morin, R, High spatial resolution detection of low-energy electrons using an event-counting method, application to point projection microscopy, *Review of Scientific Instruments* 89, 043301 (2018)

[14] – Swanson, L. W., Crouser, L. C. Total-Energy Distribution of Field-Emitted Electrons and Single-Plane Work Functions for Tungsten, *Physical Review* 163, 622 (1967)

**FIGURE AND TABLE LEGENDS:**

heat	filament	velocity	delay	pull
450	3	5	200	120
350	4	40	200	0

**Table 1:** Pulling parameters to obtain an internal-end diameter of 2 to 10 $\mu$ m with Model-P2000 from Sutter Instrument with glass capillaries B100-75-15.

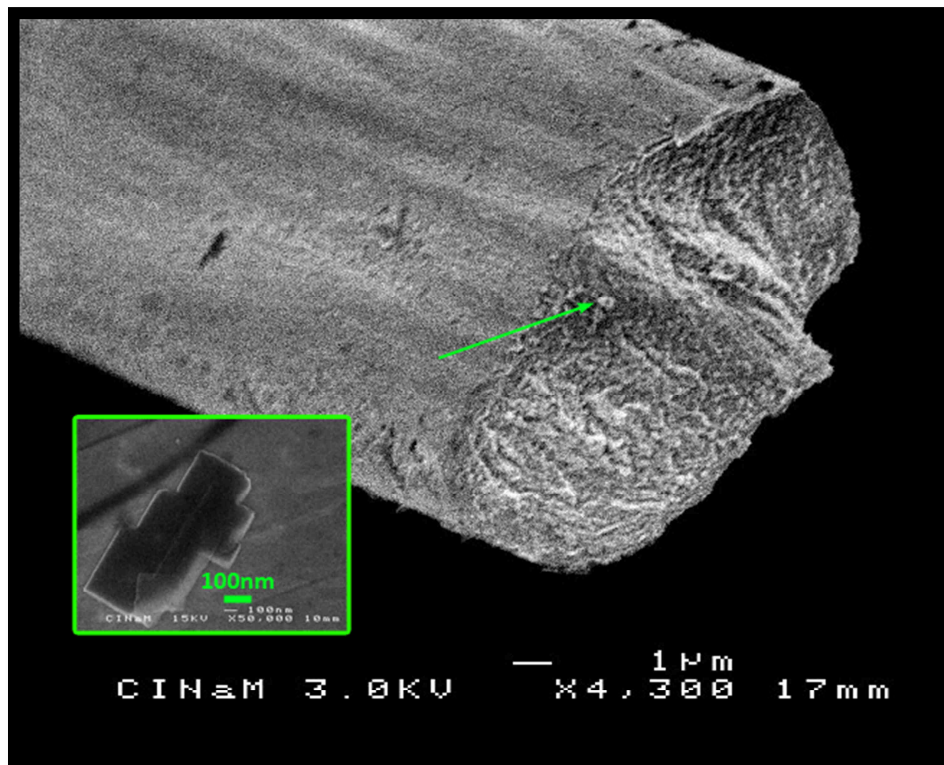


**Figure 1:** Carbon fiber with celadonite deposited on it (green arrow), observed with a scanning electron microscope. Inset: Typical close-up of a celadonite crystal.

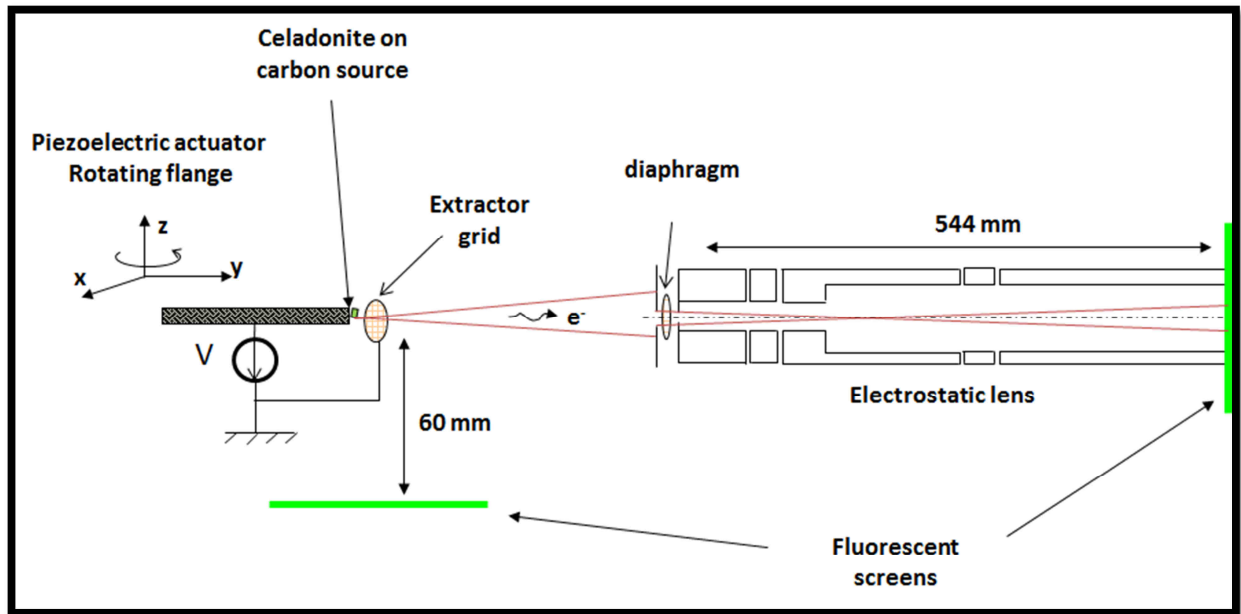


**Figure 2:** Experimental setup: the projection electron microscope using a celadonite on carbon source and an electrostatic lens; and the simple projection setup.

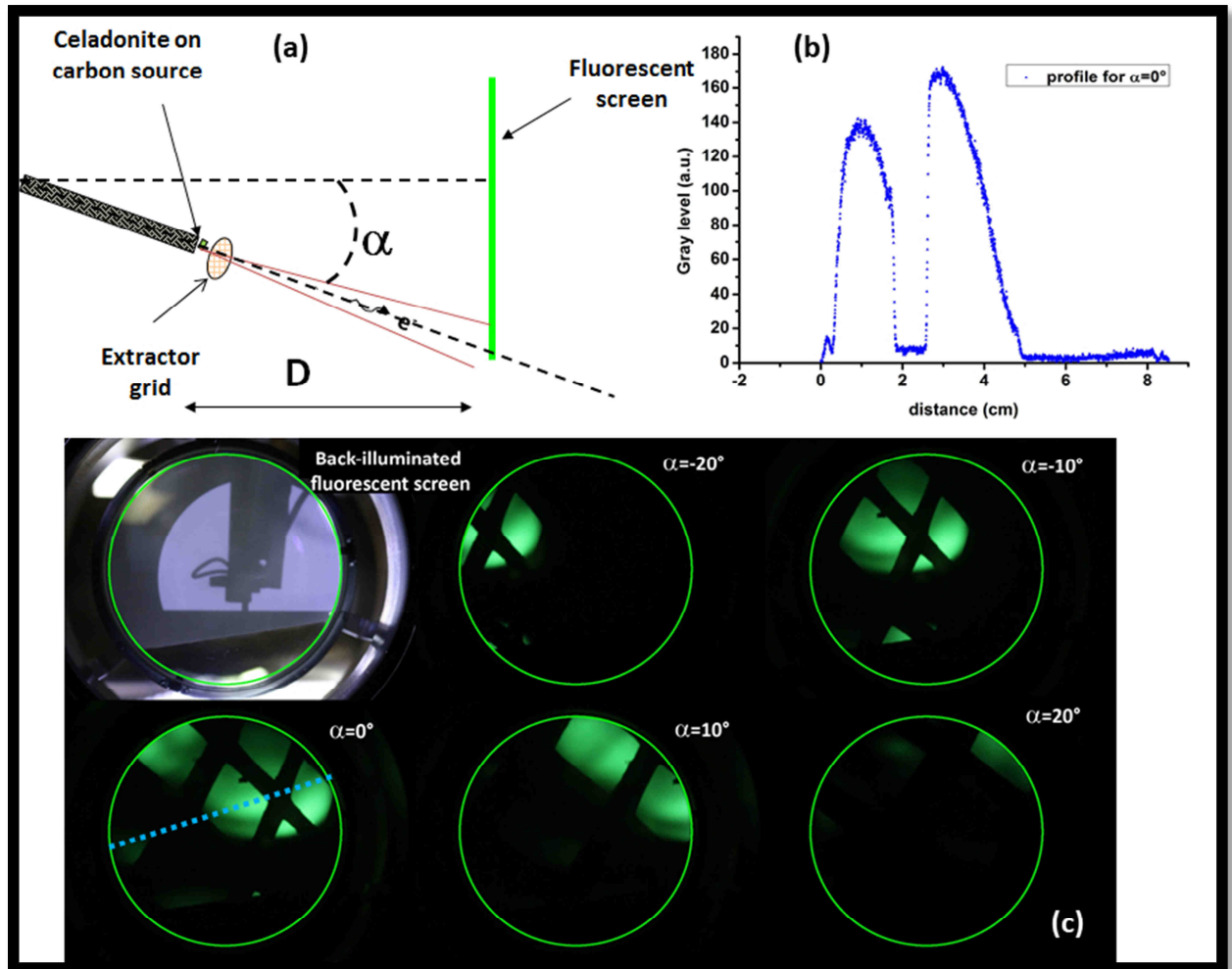


**Figure 3:** Measurement of the cone angle. (a) Schematic setup with the projection-distance  $D=5\text{cm}$  and,  $\alpha$ , the angle between the carbon fiber and the normal of the screen;  $\alpha$  is manually changed to observe the emission pattern (c) and to measure the emission profile, along the blue dashed line, obtained on the screen for  $\alpha=0^\circ$  (b). Note that the projection of the grid appears in the profile as a null intensity but clearly, the profile intensity is Gaussian with an extension of about 5 cm.

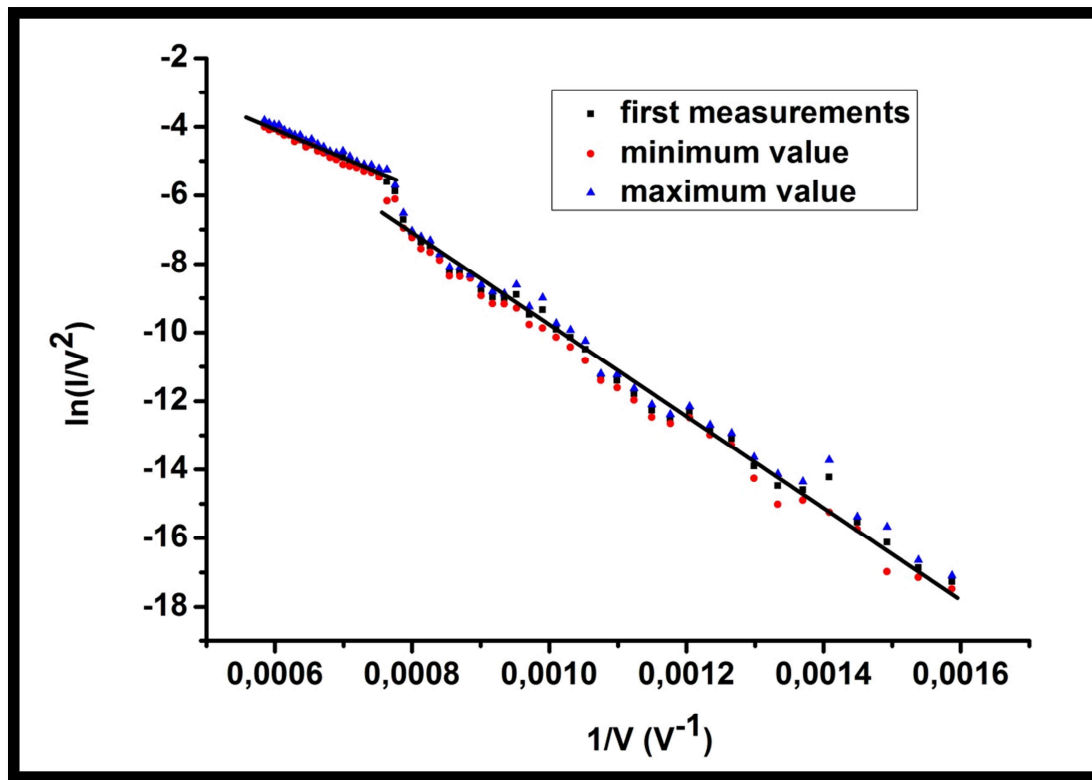


**Figure 4:** Fowler-Nordheim plot of a celadonite source

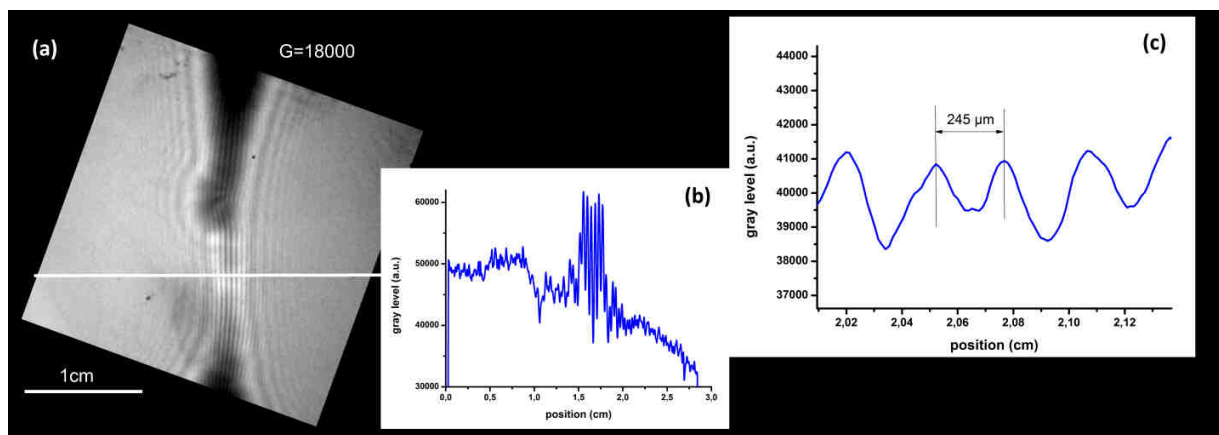


**Figure 5:** Measurement of the sharpest detail in the image to over-estimate the source size. The profile (a) is plotted along the white line in the image (a). (c) is a detail of (b).